

Pulmonary ³He MRI of Pediatric Subjects with Risk Factors for Asthma

R. V. Cadman¹, J. Dai¹, M. D. Evans², D. J. Jackson³, J. E. Gern³, R. F. Lemanske Jr.³, and S. B. Fain¹

¹Medical Physics, University of Wisconsin, Madison, WI, United States, ²Biostatistics and Medical Informatics, University of Wisconsin, Madison, WI, United States, ³Pediatrics, University of Wisconsin, Madison, WI, United States

Introduction: Assessment of pediatric lungs is usually limited to whole-lung measurements such as spirometry. Conventional lung imaging techniques expose subjects to ionizing radiation and are therefore unsuitable for longitudinal studies of children. To investigate regional patterns of obstructive disease in childhood asthma, ³He MRI, a developing lung imaging modality, was performed on 9- and 10-year-old subjects selected from a larger prospective longitudinal study of asthma. Subjects were assessed using both 3D-radial dynamic imaging with multi-echo VIPR [1] and diffusion-weighted radial stack-of-stars acquisition [2] on two separate ³He breath-holds, with I-HYPR reconstruction used for both image sequences. Imaging results were compared to clinical data from the subjects' annual visits.

Methods: MRI was performed on a 1.5-T clinical scanner (Signa HDx, GE Healthcare, Waukesha, WI) with broadband imaging capability and either a linear elliptical coil (Rapid Biomedical, Cleveland, OH) or a flexible quadrature coil (Medical Advances, Milwaukee, WI). ³He gas was polarized by spin-exchange optical pumping in a prototype commercial polarizer (GE Healthcare). During dynamic imaging, the subject was instructed to inhale a dose of ³He after the start of the scan, hold the breath for approximately 10 s, perform a rapid forced exhalation, and then breathe normally. The total acquisition time was 60 s, FOV was a 42 cm cube, and the matrix size was 128×128×128. The diffusion-weighted scan was acquired during breath hold after the subject had inhaled a second dose of ³He. This scan was a stack-of-stars acquisition with 8 phase-encoded axial slices (thickness 30 mm) and 256 radial projections. The radial projections were divided into 16 groups which alternately included or omitted a diffusion-weighting trapezoidal bipolar gradient. The bipolar gradient had timing parameters $\Delta = 2.3$ ms, $\delta = 2$ ms, and $\tau = 300$ μ s and one of eight amplitudes varying linearly from 0.238 to 1.9 G/cm, with each group of 16 projections assigned a unique amplitude.

Data from the dynamic scan were reconstructed in 1-second time frames using six iterations of the I-HYPR algorithm starting from an 8-second sliding-window composite image. A discrete score, similar to that used elsewhere [3], was used to evaluate the extent of defects observed in the reconstructed images (Fig. 1). Each defect observed was assigned a score based on the extent within its lobe: 1 if less than 25%, 2 if between 26% and 50%, 3 if between 51% and 75%, and 4 if greater than 75%. The ventilation defect score (VDS) for each lobe is the sum of the scores for all defects observed in the lobe, and the total lung VDS is the sum of the scores for each lobe. For each slice of the diffusion-weighted scan, all 256 projections were used to produce a 128×128 composite image, which was used to seed I-HYPR reconstruction to compute a separate image for each group of 16 projections. The eight unweighted images were used to create parametric maps of the combined T_1 and RF-induced relaxation. The relaxation maps were used to correct the eight weighted images, which were then fit to a Gaussian diffusion model to produce maps of the root-mean-square diffusion length X_{RMS} (Fig. 2), which is related to the size of the pulmonary air spaces. The whole-lung average X_{RMS} was computed for comparison to non-imaging metrics. VDS and average X_{RMS} were compared between groups divided based on clinical findings using analysis of variance (ANOVA) models which included a covariate for gender.

Results: Forty-four children were successfully recruited for the MRI study. Defect scores were computed from dynamic images of 43 subjects, and studies of 40 subjects were suitable for computing average X_{RMS} . The remaining studies were excluded because the subject did not maintain a sufficiently long breath hold in the case of the diffusion-weighted scan or because of technical difficulties such as inadequate ³He signal.

Results are summarized in Table 1. Asthma diagnosis at the subjects' 9- or 10-year-old clinical visit nearest to imaging was significantly correlated with both whole-lung average X_{RMS} ($p=0.02$) and VDS ($p=0.02$). Human respiratory virus (HRV) infection associated with wheezing illness prior to the third birthday was also diagnosed in this cohort. Average X_{RMS} was significantly correlated with the HRV-plus-wheezing diagnosis ($p=0.009$), but correlation between VDS and HRV-plus-wheezing did not reach significance in this cohort ($p=0.10$). A diagnosis of human respiratory syncytial virus before age 3 was not significantly correlated with either imaging metric.

Discussion and Conclusions: These results are consistent with the hypotheses that HRV infection associated with wheezing illness in early childhood leads to a narrowing of the pulmonary air spaces and that smaller spaces in the lower airways are associated with asthma. However due to the limited size and significant overlap between the group with current asthma and the group with a history of HRV-associated wheezing, it is not possible to definitively establish a causal relationship between smaller air spaces and either current asthma or wheezing history in this cohort. The measurements of ventilation defects establish that

³He MRI can be used to identify regional variations in lung function associated with asthma diagnosis in children. To improve sensitivity of the diffusion-weighting scans to multiple length scales in the lung, we are evaluating different diffusion-weighting parameters in computer and animal models. This ongoing study will include repeat ³He imaging on this cohort during adolescence.

Acknowledgements: US NIH/NCI 5T32 CA009206-31, US NIH/NHLBI P01 HL070831, and an Individual Biomedical Research Award by the Hartwell Foundation.

References: [1] Holmes JH *et al.*, Magn Reson Med 2009;62:1543-1556. [2] O'Halloran RL *et al.*, Magn Reson Med 2010;63:41-50. [3] de Lange EE *et al.*, Chest 2006;130:1055-1062.

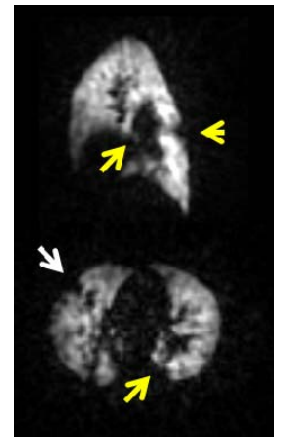


Figure 1: Two slices (sagittal on top, axial below) from the dynamic image series, with arrows indicating the locations of ventilation defects.

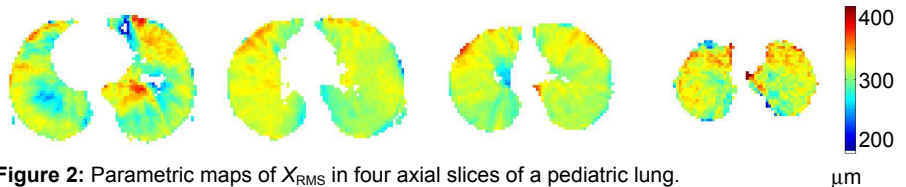


Figure 2: Parametric maps of X_{RMS} in four axial slices of a pediatric lung.

Table 1: Results.

		Average X_{RMS}			Ventilation Defect Score		
		<i>n</i>	Mean \pm SD (μ m)	<i>p</i>	<i>n</i>	Median [Q1,Q3]	<i>p</i>
Current asthma	No	23	317 \pm 21	0.02	26	6 [4, 11]	0.02
	Yes	17	302 \pm 17		17	11 [7, 22]	
HRV plus wheezing	No	24	316 \pm 22	0.009	26	6 [4, 11]	0.10
	Yes	16	301 \pm 15		17	11 [5, 22]	